Attraction Tames Two-Dimensional Melting: From Continuous to Discontinuous Transitions

Yan-Wei Li[1] and Massimo Pica Ciamarra[1,2,*]
[1]Division of Physics and Applied Physics, School of Physical and Mathematical Sciences, Nanyang Technological University, Singapore 637371, Singapore
[2]CNR–SPIN, Dipartimento di Scienze Fisiche, Università di Napoli Federico II, I-80126 Napoli, Italy

(Received 8 March 2020; accepted 7 May 2020; published 26 May 2020)

Two-dimensional systems may admit a hexatic phase and hexatic-liquid transitions of different natures. The determination of their phase diagrams proved challenging, and indeed, those of hard disks, hard regular polygons, and inverse power-law potentials have only recently been clarified. In this context, the role of attractive forces is currently speculative, despite their prevalence at both the molecular and colloidal scale. Here, we demonstrate, via numerical simulations, that attraction promotes a discontinuous melting scenario with no hexatic phase. At high-temperature, Lennard-Jones particles and attractive polygons follow the shape-dominated melting scenario observed in hard disks and hard polygons, respectively. Conversely, all systems melt via a first-order transition with no hexatic phase at low temperature, where attractive forces dominate. The intermediate temperature melting scenario is shape dependent. Our results suggest that, in colloidal experiments, the tunability of the strength of the attractive forces allows for the observation of different melting scenarios in the same system.

DOI: 10.1103/PhysRevLett.124.218002

Two-dimensional (2D) systems with short-range interactions melt either via a first-order solid-liquid transformation or via a two-step process with subsequent solid-hexatic and hexatic-liquid transitions. The two-step scenario may further follow the Kosterlitz-Thouless-Halperin-Nelson-Young (KTHNY) paradigm [1–3], with continuous solid-hexatic and hexatic-liquid transitions, or the mixed one [4], where a discontinuous hexatic-liquid transition follows a continuous solid-hexatic one. The possibly enormous value of the hexatic correlation length makes it difficult to ascertain which of the above melting scenarios a system follows. However, the increase in computational power and the development of novel algorithms, and careful experiments, allowed researchers to make progress in recent years. For instance, it is now ascertained [4,5] that, in hard disks, a discontinuous hexatic-liquid transition follows a continuous solid-hexatic one. In hard regular polygons, the melting transition depends on the number of edges, e.g., hexagons and squares following the KTHNY melting scenario and pentagons following the first-order one [6]. The melting scenario of 2D systems interacting via power-law potentials [7,8] has been demonstrated to depend on the stiffness of the interaction [9]. In these recently settled cases, density drives the melting transition, and temperature plays no role as the interaction potentials lack an energy scale.

At both the molecular and colloidal scale, attractive forces are prevalent, and the phase behavior is both temperature and density dependent. The effect of attractive forces on 2D melting remains, however, controversial. Indeed, Nelson noticed that attraction may lead to a variety of phase diagrams, illustrating possible scenarios with the hexatic phase occurring in an intermediate temperature range [10,11], for Lennard-Jones (LJ) particles. This would imply that a weak attraction promotes the hexatic phase, while a strong one suppresses it. In attractive systems, the existence of the hexatic phase is controversial, as this phase has been observed in some studies [12,13], but not in others [14,15]. The complete mapping of the phase diagram of LJ particles is a recent, but still debated, achievement [16]; indeed, at high-temperature, where attractive forces are negligible, LJ particles have been found not to follow the melting scenario of $1/r^{12}$ [9,16] ones.

Here, we demonstrate, via the numerical determination of the temperature-density phase diagram of attractive hexagons, pentagons, squares, and LJ point particles, that attraction universally influences the melting scenario by suppressing the hexatic phase and promoting discontinuous transitions.

We simulate attractive hexagons ($N = 48\,071$), pentagons ($N = 20\,449$) and squares ($N = 20\,521$), as well as Lennard-Jones point particles ($N = 318^2$), under periodic boundary conditions, in the canonical ensemble using the graphics processing unit-accelerated GALAMOST package [17]. We construct the extended polygons by lumping together LJ point particles equally spaced along the perimeter, as shown in Fig. S1 [18]. The resulting short-ranged attractive interaction, detailed in the Supplemental Material [18], allows estimating the size of the polygonal particles and their interaction energy scale, we adopt as our

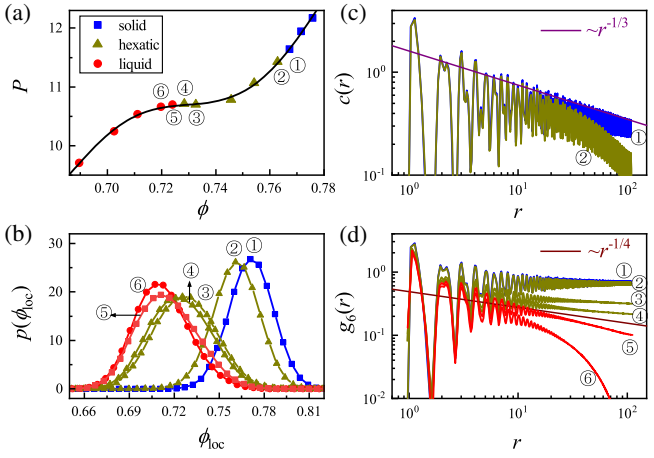

FIG. 1. High-temperature melting of attractive hexagons (a) Equation of state at $T = 1.40$. Different symbols correspond to different phases, as illustrated in the legend. The black line is a fifth-order polynomial fit. (b) The local density histograms, (c) the translational correlation function $c(r)$, and (d) the bond-orientational correlation function $g_6(r)$ for different densities, as indicated in (a).

units of length and energy, respectively. For the considered state points and interaction, the values of N we consider are large enough for finite-size effects to be negligible, as we prove in Fig. S3 in the Supplemental Material [18]. We verify thermal equilibration by ascertaining that the same final state is reached in simulations starting from a liquid-like configuration and an ordered one, as illustrated in Fig. S2 [18].

Attractive hexagons at high temperatures.—We begin by reporting results for the determination of the phase diagram of attractive hexagons. At high temperature, the pressure of attractive hexagons increases monotonically with the density, as illustrated in Fig. 1(a). We associate to each particle a local density defined as $\rho(\vec{r}_i) = \{[\sum_{j=1}^{N} H(r_c - |\vec{r}_i - \vec{r}_j|)]/\pi r_c^2\}$, where H is the Heaviside step function, $r_c = 50$. Results are robust with respect to choice of r_c, unless it becomes very small, or of the order of the system size. Figure 1(b) shows the distribution of the local density, which is always unimodal. The density dependence of the pressure and of the local density distribution exclude the presence of a discontinuous transition with a coexistence phase. We identify the different pure phases investigating the spatial decay of the correlation function of the translational, $c(r)$, and of the bond-orientational order, $g_6(r)$. The translational correlation function is $c(r = |\vec{r}_i - \vec{r}_j|) = e^{i\vec{G}\cdot(\vec{r}_i - \vec{r}_j)}$, where $\vec{G}$ is one of the first Bragg peaks, identified by the static structure factor [4,19]. The bond-orientational correlation function is $g_k(r = |\vec{r}_i - \vec{r}_j|) = \langle \psi_k(\vec{r}_i)\psi_k^*(\vec{r}_j)\rangle$, where $\psi_k(\vec{r}_i)$ is the bond-orientational order parameter of particle i, defined as $\psi_k(\vec{r}_i) = (1/n)\sum_{m=1}^{n} \exp(ik\theta_m^i)$. Here, n is the number of nearest neighbors of the particle and θ_m^i is the angle between $(\vec{r}_m - \vec{r}_i)$ and a fixed arbitrary axis. The value of k reflects the rotational symmetry of the crystal structure: $k = 4$ for squares, $k = 6$ for the other particles.

At high density, the system is in the solid phase. Consistently, we observe the translational correlation function to decay as $c(r) \propto r^{-\eta}$ with $\eta \leq 1/3$, a consequence of the Mermin-Wagner theorem [20], and the bond-orientational correlation function to reach a constant, as illustrated in Figs. 1(c) and 1(d) for state point ①;. At lower density, $c(r)$ decays exponentially, while $g_6(r)$ has a power-law decay, $g_6(r) \propto r^{-\eta_6}$ with $\eta_6 < 1/4$. This occurs, for instance, at state points ②–④, and indicates that the system is in the hexatic phase. Further lowering the density, the system enters the liquid phase, where both correlation functions decay exponentially.

These findings demonstrate that, at high temperature, LJ hexagons follow the KTHNY scenario [1–3]. This result agrees with a previous investigation of the melting transition of hard hexagons [6], the role of attractive forces being negligible at high temperatures.

Attractive hexagons at intermediate temperature.—As the temperature decreases, the equation of state of attractive hexagons flattens in a range of densities and develops a Mayer-Wood [21] loop for $T \lesssim 0.53$, as illustrated in Fig. 2(a). Since pressure loops are induced by the interfacial free energy of coexisting phases [4,22], this indicates the presence of a first-order transition. Within the coexisting region, the distribution of the local density becomes extremely broad and well described by the superposition of two Gaussian functions, as shown in Fig. 2(b). Besides, the distribution becomes system-size dependent, with a bimodal character more apparent in larger systems, as we show in Fig. S3 [18]. These findings further support the presence of coexisting phases.

We determine the coexistence boundaries via the Maxwell construction with the pressure curve fitted by either a fifth- or a tenth-order polynomial. Outside of the coexistence region, we identify the pure phases investigating the translational and the bond-orientational correlation functions, as summarized in Figs. 2(c) and 2(d). We observe the solid phase (e.g., ①), where $c(r)$ decays algebraically and $g_6(r)$ is extended, the hexatic phase (e.g., ②), where $c(r)$ decays exponentially and $g_6(r)$ is extended, and the liquid phase (e.g., ⑦) where both correlation functions decay exponentially. These results indicate that, at intermediate temperatures, attractive hexagons follow the mixed melting scenario with a continuous solid-hexatic transition anticipating a discontinuous hexatic-liquid transition.

We visualize the different phases by color coding each particle according to the angle $\Delta\alpha_k^i$ between the global $\vec{\Psi}_k = (1/N)\sum_i \psi_k(\vec{r}_i)$ and the local $\psi_k(\vec{r}_i)$ bond-orientational parameters, $\psi_k(\vec{r}_i) \cdot \vec{\Psi}_k^* = |\psi_k(\vec{r}_i)||\vec{\Psi}_k^*| \cos(\Delta\alpha_k^i)$. In the solid and hexatic phase, the long-range or quasi-long-range nature of the bond-orientational order leads to

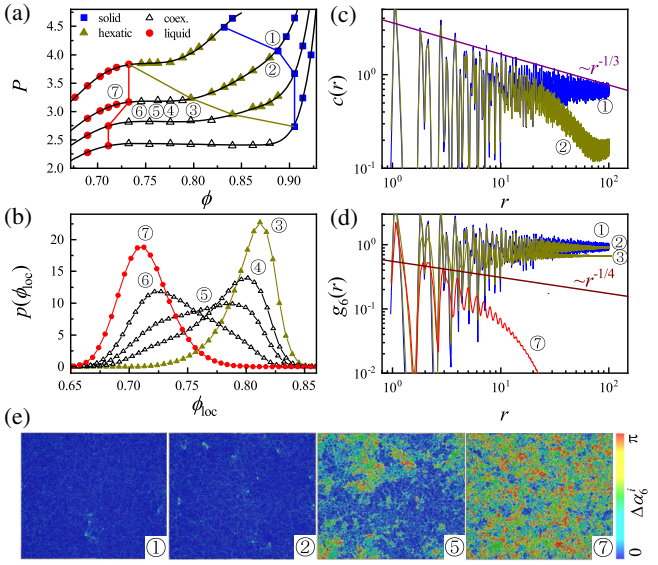

FIG. 2. Intermediate-temperature melting of attractive hexagons. (a) Equation of state at $T = 0.60$, 0.53, 0.49, and 0.46, from top to bottom. Different symbols correspond to different phases, as illustrated in the legend. The black lines are from polynomial fits. Phase boundaries are marked by the red, dark yellow, and blue lines. (b) Local density distributions, (c) translational and (d) bond-orientational correlation functions, and (e) snapshots of the system at $T = 0.53$, for different densities. In (e) each hexagon is color coded according to the angle between its local bond-orientational parameter, and the global one.

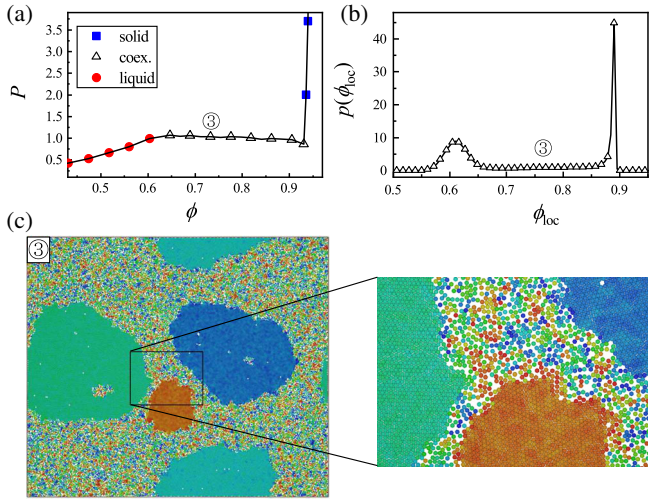

FIG. 3. Low-temperature melting of attractive hexagons. (a) Equation of state at $T = 0.35$. The black line is a guide to the eyes. (b) Local density distributions at a density value within the coexistence region. (c) Snapshot of the whole system (left), and enlargement of part of it (right), at the corresponding value of the density. The color code is as in Fig. 2(e).

snapshots with a uniform color, as in Fig. 2(e) ①and ②;. In the liquid phase, Fig. 2(e) ⑦, the snapshot appears almost randomly colored, due to the short-range of the bond-orientational order. In the coexistence phase, Fig. 2(e) ⑤, the coexistence of hexatic and liquid phases lead to that of regions of uniform color and regions randomly colored.

Attractive hexagons at low temperature.—As the temperature decreases, the coexistence region widens, and the hexatic phase shrinks, as is apparent in Fig. 2(a). At low enough temperatures, therefore, melting occurs via a first-order liquid-solid transition with no hexatic phase. The pressure loop and the bimodal character of the local density distribution within the coexistence region, which we illustrate in Fig. 3, confirms that the system undergoes a discontinuous transition at low temperature.

Furthermore, snapshots of the system indicate that the coexisting phases are of solid and liquid type, as in Fig. 3(c). Therefore, we can exclude an intermediate hexatic phase, further supporting a first-order melting scenario at low temperature.

Shape and temperature dependence of the melting scenario.—The phase diagram of Fig. 4(a) summarizes the results we have obtained so far: for attractive hexagons, melting is of KTHNY type at high temperature and becomes, first, of mixed type and, then, first-order as the temperature decreases. The system has no liquid-gas transition, nor a solid-solid transition, as the attraction range, we determine in Table I in the Supplemental Material [18], is small but not much smaller than the particle size. This suppresses the liquid-gas critical point [23] without promoting a solid-solid transition [23–25]. In the solid, the body orientation of the hexagonal particles is long ranged, thus, excluding the presence of a plastic-crystal phase.

We investigate the universality of the role of attraction in the 2D melting by determining the phase diagram for different particle shapes: squares, pentagons, and LJ point particles (disks). Squares crystallize in the square lattice, all other shapes in the hexagonal one. For pentagons, shape frustration is not able to inhibit crystallization at the lowest temperature ($T = 0.19$) and the highest density ($\phi = 0.854$) we studied. Details on the phase determination are in Figs. S4 and S5 [18], for squares and pentagons, and elsewhere for disks [26]. The resulting phase diagrams are in Figs. 4(b)–4(d).

At high temperature, the polygonal particles follow the melting scenario previously reported for hard particles [6], KTHNY for squares and first-order for pentagons. LJ disks follow the mixed scenario as r^{-12} particles [9]. As in hexagons, in both squares and pentagons, the liquid-gas transition is suppressed, and no plastic-crystal phase occurs. In LJ disks, the liquid-gas critical point occurs at low temperature and low density, well outside the parameter space we have investigated.

Regardless of the high-temperature behavior, melting always occurs via a first-order solid-liquid transition at low temperature, and the coexistence region broadens as the temperature decreases. These findings imply that particles'

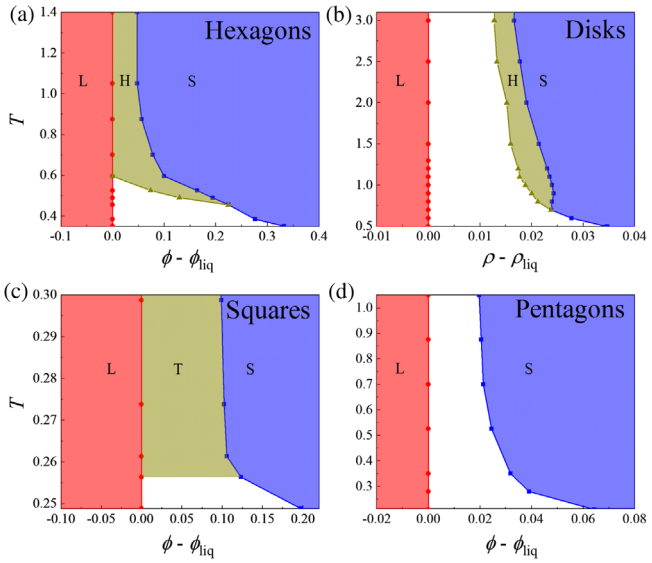

FIG. 4. Phase diagram of attractive polygons and LJ disks. The phase diagrams for (a) hexagons, (c) squares, and (d) pentagons are plotted in the T-$\phi - \phi_{liq}$ plane and the one for (b) disks is in T-$\rho - \rho_{liq}$ plane, where ϕ_{liq} (ρ_{liq}) is the highest area fraction (number density) of the liquid phase. At each investigated temperature, we mark the estimated phase boundaries with symbols. Colors are used to distinguish the pure phases, liquid (L), solid (S), hexatic (H), and tetratic (T). Coexistence regions, including hexatic-liquid and solid-liquid coexistence, are white. The corresponding phase diagrams in the T-ϕ (or T-ρ) plane are in Fig. S6 [18].

shapes fix the melting scenario at high temperature, attractive forces at low temperatures. At intermediate temperatures, conversely, both shape and attraction may be relevant. In disks, the hexatic phase disappears as the temperature decreases, making the melting transition first order. In squares, the equation of state within the tetratic region becomes flat as the temperature decreases without the coexistence region shrinking, as we illustrate in Fig. S4 [18]. Hence, no intermediate mixed scenario separates the high-temperature continuous melting and the low-temperature discontinuous one. In this respect, squares differ from hexagons and disks. In pentagons, the transition is always first order.

These results consistently demonstrate that attraction influences the melting scenario of 2D systems by promoting the emergence of a coexistence region, if this is not already present in the high-temperature limit, as well as widening it. The widening of the coexisting region leads to the disappearance of the hexatic-tetratic phase and, hence, to a first-order melting transition.

Conclusions.—Different system properties affect the melting scenario in 2D [6,9,27–29]. In this context, the influence of attractive forces was unclear, despite their prevalence at both the molecular and colloidal scale. We have found that attractive forces induce a discontinuous transition and widen the coexistence region at the expense of the hexatic phase, making the low-temperature melting transition first order. Hence, attractive forces never induce the hexatic phase or widen the hexatic region, at variance with previous speculations [10,11]. We suggest that attractive forces always promote the discontinuous transition, as we demonstrated this occurring in systems which melt according to different scenarios at high temperature.

Theoretically, our results suggest that the dislocation core energy, E_c, is suppressed at low temperatures in the presence of attractive forces. Conversely, at low temperature, $E_c/k_bT \gg 1$, and a continuous two-step melting scenario may occur, according to the KTHNY theory. We are looking forward to the experimental investigation of our predictions in colloidal systems, where the tuning of the strength of the attractive forces, e.g., via the depletion interaction, should allow for the observation of different melting scenarios in the same system, e.g., colloidal hexagonal-shaped particles.

The interparticle interaction of our polygonal particles inherits their discrete rotational symmetry, as the attraction range is small compared to the particle size, as we detail in the Supplemental Material [18]. As the attraction range increases, this discrete rotational symmetry vanishes and the interaction becomes more rotationally symmetric. Hence, while we have not explicitly investigated the role of the attraction range on the phase behavior, we anticipate that, on increasing the attraction range, the phase diagrams of the polygonal particles evolve toward that of the LJ point particles.

We acknowledge support from the Singapore Ministry of Education through the Academic Research Fund No. MOE2017-T2-1-066 (S), and are grateful to the National Supercomputing Centre (NSCC) of Singapore for providing computational resources. We thank Joyjit Chattoraj for helpful discussions.

*massimo@ntu.edu.sg

[1] J. M. Kosterlitz and D. J. Thouless, J. Phys. C **6**, 1181 (1973).
[2] B. I. Halperin and D. R. Nelson, Phys. Rev. Lett. **41**, 121 (1978).
[3] A. P. Young, Phys. Rev. B **19**, 1855 (1979).
[4] E. P. Bernard and W. Krauth, Phys. Rev. Lett. **107**, 155704 (2011).
[5] A. L. Thorneywork, J. L. Abbott, D. G. A. L. Aarts, and R. P. A. Dullens, Phys. Rev. Lett. **118**, 158001 (2017).
[6] J. A. Anderson, J. Antonaglia, J. A. Millan, M. Engel, and S. C. Glotzer, Phys. Rev. X **7**, 021001 (2017).
[7] C. C. Grimes and G. Adams, Phys. Rev. Lett. **42**, 795 (1979).
[8] P. Keim, G. Maret, and H. H. von Grünberg, Phys. Rev. E **75**, 031402 (2007).
[9] S. C. Kapfer and W. Krauth, Phys. Rev. Lett. **114**, 035702 (2015).

[10] D. R. Nelson and B. I. Halperin, Phys. Rev. B **19**, 2457 (1979).
[11] D. R. Nelson, *Defects and Geometry in Condensed Matter Physics* (Cambridge University Press, Cambridge, England, 2002).
[12] K. Wierschem and E. Manousakis, Phys. Rev. B **83**, 214108 (2011).
[13] H. Shiba, A. Onuki, and T. Araki, Europhys. Lett. **86**, 66004 (2009).
[14] D. Du, M. Doxastakis, E. Hilou, and S. L. Biswal, Soft Matter **13**, 1548 (2017).
[15] B. Li, X. Xiao, S. Wang, W. Wen, and Z. Wang, Phys. Rev. X **9**, 031032 (2019).
[16] A. Hajibabaei and K. S. Kim, Phys. Rev. E **99**, 022145 (2019).
[17] Y. Zhu, H. Liu, Z. Li, H. Qian, G. Milano, and Z. Lu, J. Comput. Chem. **34**, 2197 (2013).
[18] See Supplemental Material at http://link.aps.org/supplemental/10.1103/PhysRevLett.124.218002 for additional information about the interparticle interaction, unit, thermal equilibration, finite-size effects, phase determination for squares and pentagons, and the phase diagram in T-ϕ plane.
[19] Y.-W. Li and M. P. Ciamarra, Phys. Rev. E **100**, 062606 (2019).
[20] N. D. Mermin and H. Wagner, Phys. Rev. Lett. **17**, 1133 (1966).
[21] J. E. Mayer and W. W. Wood, J. Chem. Phys. **42**, 4268 (1965).
[22] H. Furukawa and K. Binder, Phys. Rev. A **26**, 556 (1982).
[23] P. Bolhuis and D. Frenkel, Phys. Rev. Lett. **72**, 2211 (1994).
[24] P. Bladon and D. Frenkel, Phys. Rev. Lett. **74**, 2519 (1995).
[25] M. Dijkstra, Phys. Rev. E **66**, 021402 (2002).
[26] Y.-W. Li and M. P. Ciamarra (to be published).
[27] Y.-W. Li and M. P. Ciamarra, Phys. Rev. Mater. **2**, 045602 (2018).
[28] J. Russo and N. B. Wilding, Phys. Rev. Lett. **119**, 115702 (2017).
[29] M. Zu, J. Liu, H. Tong, and N. Xu, Phys. Rev. Lett. **117**, 085702 (2016).